SIMULATION OF S-CO_2 INTEGRATED SYSTEM TEST WITH ANL PLANT DYNAMICS CODE

Anton Moisseytsev
Principal Nuclear Engineer
Argonne National Laboratory
Argonne, IL USA
amoissey@anl.gov

James J. Sienicki
Manager, Innovative Systems and Engineering Assessments
Argonne National Laboratory
Argonne, IL USA
sienicki@anl.gov

Anton Moisseytsev is a Principal Computational Nuclear Engineer in the Nuclear Engineering Division of Argonne National Laboratory (ANL). He has twelve years of experience in modeling and simulation of various systems, including design and analysis of the advanced reactors and energy conversion systems, safety analysis of nuclear reactors, and code development for steady-state and transient simulations of nuclear power plants. Anton has been involved in the development of the supercritical carbon dioxide Brayton cycle at Argonne since 2002.

James J. Sienicki is the Manager of the Innovative Systems and Engineering Assessments Section and a Senior Nuclear Engineer in the Nuclear Engineering Division at ANL. He has been leading the development of the supercritical carbon dioxide Brayton cycle at ANL with funding from the U.S. Department of Energy since 2002. He is involved in the design of S-CO_2 Brayton cycle power converters for Sodium-Cooled Fast Reactors as well as the design and analysis of experiments on fundamental phenomena involved in heat exchangers for supercritical CO_2 cycles.

ABSTRACT

The Plant Dynamics Code (PDC) has been developed at Argonne National Laboratory for system level transient analysis of supercritical carbon dioxide (S-CO_2) Brayton cycle power converters. Current code activities are focused on testing and validation using available experiment data from small-scale S-CO_2 Brayton cycle demonstrations. One such demonstration is the S-CO_2 Integrated System Test (IST) facility at the Bechtel Marine Propulsion Corporation (BMPC) which is a 100 kWe simple recuperated Brayton cycle configuration focused on performance modeling and power level control method development. For this work, BMPC has provided ANL with a set of steady-state and transient experiment data from the IST. Results of simulation of the IST with the PDC are presented. Good agreement is obtained for both the steady-state and transient conditions.

INTRODUCTION

As development of the supercritical carbon dioxide (S-CO_2) Brayton cycle progresses in the United States and elsewhere in the world (e.g., Republic of Korea, France, Japan, and the Czech Republic), more and more experimental data sets are becoming available that demonstrate the performance of S-CO_2 as a supercritical Brayton cycle working fluid and enable testing and validation of analysis computer codes. Code testing and validation is a critical step to confirm the credibility of codes when they are applied to predict the performance of full-size S-CO_2 commercial power and marine propulsion systems. Since such full-scale S-CO_2 systems have not been built and tested yet, using the analytical codes is the only way currently available to predict system performance and confirm the benefits for power plant and propulsion applications. At the same time, the S-CO_2 cycles have unique features which require the analytical codes to accurately address such features in order to be used as reliable performance prediction tools. The unique code features can be validated against the experimental data currently becoming available from the small-scale S-CO_2 experiments provided that the experiment conditions are sufficiently prototypical of the full-size systems.

An integral S-CO_2 cycle demonstration in operation in the U.S. is the S-CO_2 cycle Integrated System Test (IST) operated by Bechtel Marine Propulsion Corporation. A detailed description of the IST is provided in Clementoni and Cox, 2014a and 2014b; Kimball, 2014; and Rahner, 2014. Selected IST data were recently shared with Argonne National Laboratory (ANL) as a benchmark exercise, which allows extending the validation base for the ANL Plant Dynamics Code.

The Plant Dynamics Code (PDC) has been developed at Argonne National Laboratory for system level transient analysis of S-CO_2 Brayton cycle power converters (Moisseytsev and Sienicki, 2006). The code has been used extensively for cycle design analysis, as well as for development and refinement of cycle control strategies. Recently, testing and validation of the PDC code has been focused on comparing code predictions with the experimental data obtained at the Sandia National Laboratories (SNL) Recompression Closed Brayton Cycle (RCBC) S-CO_2 Loop (Moisseytsev and Sienicki, 2015). Extending the PDC validation base to include the IST data is significant because of several specific and different features of the IST compared to the SNL loop.

Benefits of IST Data for S-CO_2 Codes Validation

For code testing and validation purposes, the IST data present several benefits in comparison, and in addition, to the SNL RCBC data.

First, this dataset provides diversity in the experimental data. Even though several features of the SNL and BMPC loops are similar, such as the common design of the turbomachinery components, there are sufficient differences in the loops' designs and operation, which allow concentrating the validation effort on sufficiently different models and/or conditions of the S-CO_2 cycle design and analysis. The most important such features of the IST loop include:

- The IST loop was *designed to be operated and is operated* further from the CO_2 critical point than the SNL loop, which reduces the effects of phenomena due to potential property uncertainties in the code models at compressor inlet conditions, which, in turn, reduces the uncertainty of the model prediction of such conditions, both for the design and performance prediction of the main cycle components. Thus, the effects of other phenomena that remain away from the critical point take on a greater relative significance. On the other hand, lack of data close to the critical point excludes testing and validation of code features designed to predict the cycle performance closer to the critical point.
- The IST loop operators were able to conduct the experiments over a long duration. One of the datasets provided to ANL is for a run duration of about two hours, with around one hour of no-extra-control operation to achieve approximate steady-state conditions. The near steady-state data are helpful for refining of component models, specifically, the heat exchangers, when comprehensive and detailed design information for these components is not available.
- The IST loop employs shell-and-tube heat exchangers for the heat source and heat sink heat exchangers. The design and, therefore, the modeling of this type of the heat exchangers is simpler than for the Printed Circuit Heat Exchangers (PCHEs) used in the SNL loop, because fewer design parameters exist. In addition, the internal configuration of these heat exchangers is better known, while the internal design of a PCHE is proprietary manufacturer information.
- The IST loop uses an external oil loop to provide heat to the S-CO_2 cycle, compared to the direct electrical heaters in the SNL loop. This configuration with an oil loop and oil-to-CO_2 heat exchanger is more prototypical of reactor applications that would use reactor-fluid-to-CO_2 heat exchangers.
- The IST loop has thermal insulation on all pipes and components, in contrast to the SNL loop.

- The IST benchmark specifications include more detailed loop information than has been available thus far for the SNL loop. For example, manufacturer data for the valves and flow meters, including pressure drop estimates and measurements, were provided with the benchmark.

IST EXPERIMENTAL DATA

IST Loop Configuration

The IST test referred to as P1-S2-63264-CC_7000s was analyzed. This test was selected because of the long operation (for 7000 s) to achieve near steady-state conditions. The IST configuration for this test is shown in Figure 1. There are two turbomachinery shafts, one for the compressor, alternator and turbine (referred to as “compressor turbine”); the other shaft is for the generator and the generator turbine. The heat is added to the cycle in the oil-to-CO_2 intermediate heat exchanger (IHX). The PDC model of the IST described in this paper models the oil loop only to provide the boundary conditions for the CO_2 cycle. To that end, the entire oil loop is not modeled. Only the oil side of the IHX is modeled in the PDC, while the oil flow rate and inlet temperature to the IHX are provided to the model as inputs.

After the IHX, the CO_2 flow is split between the main flow and the turbine bypass, and then again between the two turbines. The flow splits can be controlled by two valves upstream of each turbine and the bypass valve. After the turbines, the flows are combined before entering the hot side of the recuperator. The flow then enters the precooler and is sent to the compressor. After the compressor, the flow passes through the low temperature side of the recuperator before returning to the IHX inlet.

The IST also incorporates a compressor recirculation valve to take some flow from the compressor outlet and send it to the precooler inlet bypassing the rest of the loop. This valve is controlled by means of a pre-programmed lookup table of requested valve position versus commanded compressor speed.

Figure 1 also shows the seal leakage flows which are collected from both shafts and returned to the loop upstream of the precooler.

The valves are shown in Figure 1 as circles, and the split/merge points (tee’s) are shown as triangles.

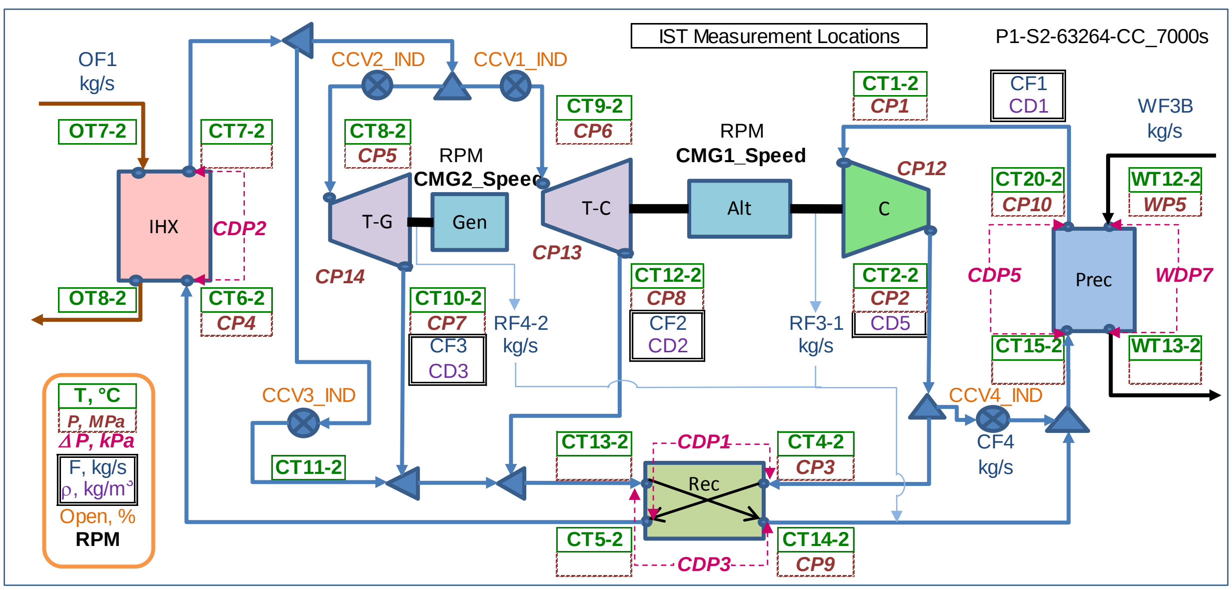

Figure 1. IST Configuration for P1-S2-63264-CC_7000s Test.

In addition to the loop configuration, Figure 1 also indicates the measurement sensor locations throughout the loop. The meaning of each sensor is defined in the legend in the bottom-left corner in Figure 1.

The benchmark package provided by BMPC included: measured data at 1 Hz frequency for all available measurements, manufacturer specification sheets for the IHX and precooler heat exchangers (each sheet includes, among other information, the tube dimensions, tube count, and some design information on the baffle plates), manufacturer specification sheets for the valves, piping layout and dimensions, piping and instrumentation diagram (P&ID) showing the location of the sensors, description of a BMPC TRACE thermal hydraulics model of the recuperator, showing the flow area, hydraulic diameter, channel length, and other parameters assumed in the model, oil properties tables, and test description.

Test P1-S2-63264-CC_7000s

Test P1-S2-63264-CC_7000s was selected from two tests supplied with the benchmark specifications for the current analysis because of its better near steady-state data. The test was run for 7,000 seconds, of which in the last 3,500 seconds, no external control action was introduced allowing one hour of system stabilization toward a steady state.

The rotational speed for both shafts was initially set to 37,500 rpm. The turbine-generator shaft speed was changed to 55,000 rpm at 346 seconds and was held constant for the rest of the test. The turbine-compressor shaft speed was changed in several steps from 37,500 rpm to 55,000 rpm. The last change in the shaft speed was commanded at 3565 seconds.

The turbine throttling valves were set to 100% and the turbine bypass valve was 0% for the entire test. The compressor recirculation valve is controlled by a lookup table dependent on the commanded compressor speed. For the speeds of 37,500 to 55,000 rpm in this test, the valve position varied from 70% open to 50% open.

The turbomachinery cavity pressure is initially set to 400 psia (2.76 MPa) and was changed to 300 psia (2.07 MPa) at 78 seconds. The oil loop conditions are set by automatic control to maintain a 540 °F (282.2 °C) CO_2 temperature at the IHX outlet. The oil flow rate is set to a constant 50 lbm/s (22.7 kg/s). The compressor-inlet temperature is set to 96 °F (35.6 °C) by means of the water flow rate control. The water temperature at the precooler inlet is controlled at 80 °F (26.7 °C).

The as-measured experimental conditions at 7,000 seconds are shown in the bottom plot of Figure 2.

Measurement Uncertainties

The first two columns of Table 1 list the measurement uncertainties as provided by BMPC. These values represent the acceptance basis for the calibration check of each sensor. There are, however, reasons to believe that the overall measurement uncertainties in the data are larger than those in the “sensor” column of Table 1. First, only one measurement is made for each location. There is no redundancy in the IST measurements. So, if there is any property distribution, say, inside a pipe, this distribution will not be captured in any way by the data acquisition system. Also, the measurements are made at some distance (5 inches or so) from the actual component inlet and outlet. In the modeling, comparison is made with the exact inlet/outlet locations. Although the effects of this difference are believed to be small, they will still contribute to differences between the model predictions and the experimental data.

The turbomachinery shaft cavity leakage flow collection system uses recirculating piston pumps to re-inject seal leakage flow back into the main loop. The pumps operate at about one stroke per 4 seconds. So, the system parameters, especially pressure near the reinjection point (which includes the locations around the recuperator and the precooler), will show some oscillations with about a 4 second period. To address this feature, the experimental data for each measurement were averaged over 10 seconds for the comparison with the PDC steady-state (but not transient) predictions. Compared to instantaneous readings, there are some differences resulting from such data averaging. Also, the absolute values of the standard deviation of the data during the averaging interval were calculated. In most cases, these deviations are small, but still at least comparable to the stated sensor accuracy. For example, the compressor-inlet pressure deviation of 0.013 MPa (or 0.13%) doubles the sensor uncertainty. The compressor-inlet temperature deviation of 0.03 °C translates to 0.08%, which is about one-half of the sensor uncertainty. In some locations, however, the difference is much higher. The flow rate at the compressor turbine outlet, for example, shows a deviation of 0.0124 kg/s, which is equal to 0.6% of the 1.9228 kg/s measured value. This fluctuation is 20 times higher than the stated flow measurement uncertainty. The cold side recuperator outlet temperature and precooler inlet temperature show deviations of 0.66 °C and 0.23 °C, which translates to 0.3% and 0.5% of the measured temperature, respectively.

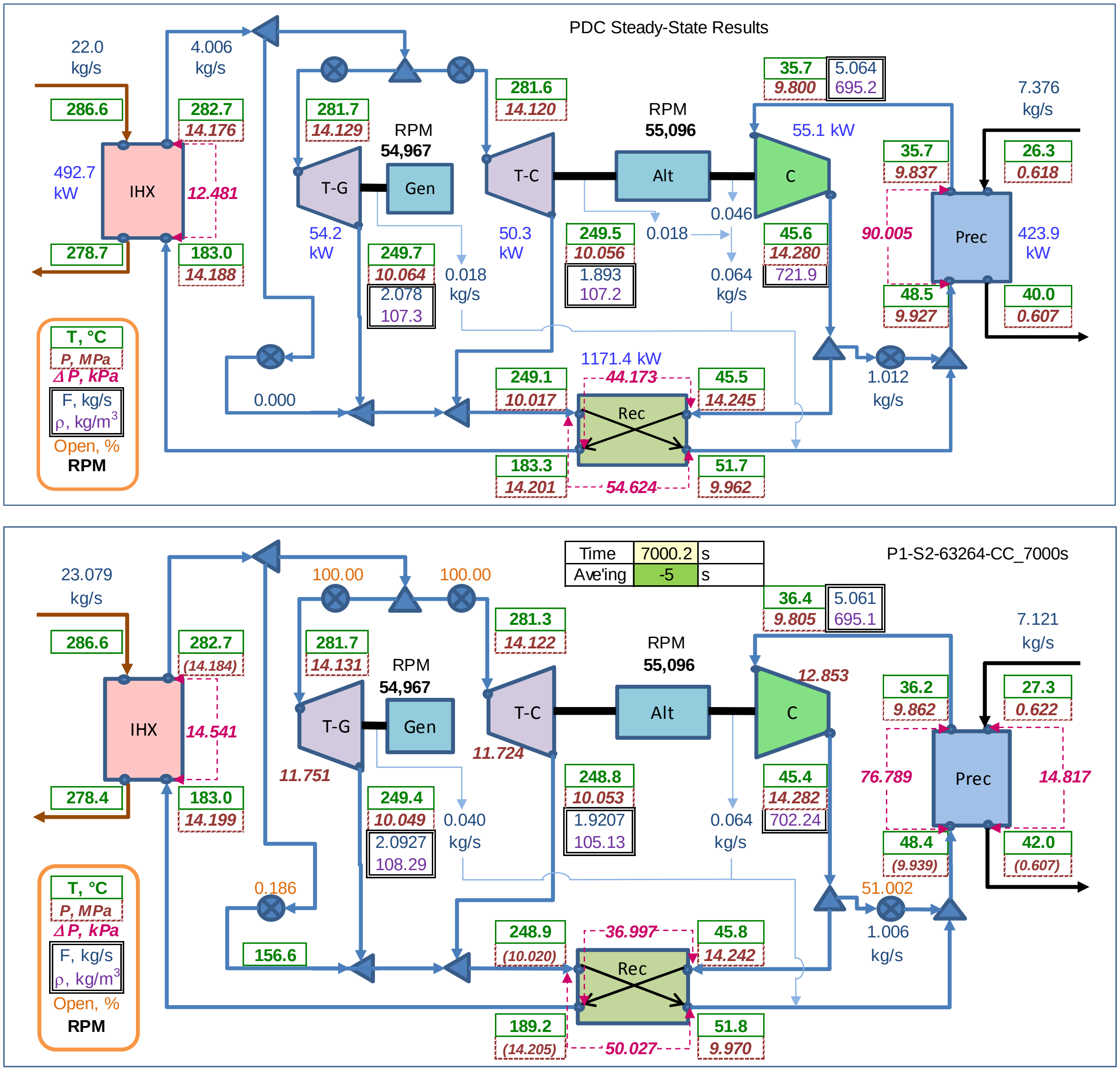

Figure 2. PDC Steady-State Results (Top) Compared to the Test Data (Bottom).

There are also some inconsistencies in the experimental data. There is 0.4 °C temperature *increase* between the compressor and the recuperator, which is much higher than the stated measurement uncertainty. Also, there is a significant temperature drop, 5.9 °C, between the recuperator and the IHX, which is much larger than what can be explained by the heat losses in the pipe.

Another observation of the data is related to the compressor-inlet conditions which are important to the modeling of the loop. When National Institute of Standards and Technology (NIST) CO_2 properties (NIST, 2015) are applied to the measured pressure and temperature, a density of 684.8 kg/m^3 is calculated, which is 1.5% lower than the measured value of 695.1 kg/m^3.

The experimental data were measured at the end of long near steady-state operation. As such, they should represent conditions at least close to steady-state. One way to check if steady-state conditions are reached is to compare the heat balances on two sides of the heat exchangers. This comparison for the

IHX, recuperator, and precooler shows that the heat balance is achieved all heat exchangers *only* if a measurement uncertainty of 1 °C is assumed.

Because of all the previous discussion, it is believed that the uncertainties listed in the "sensor" column of Table 1 do not capture all the uncertainties for each measured value. The larger uncertainties adopted for this paper are presented in in the "total" column of Table 1. These values represent the combination of all sources of uncertainties discussed above and will be used in this paper when the model prediction is compared to the experimental results.

Table 1. Specified Uncertainties for the Sensors

Measurement	Sensor Uncertainty	Total Uncertainty
Mass Flow Rate and Density	±0.1% of measured value	±1% of measured value
Temperature	±0.4% of measured value (in °C)	±1°C
Pressure	±0.625% of measured value	±1% of measured value
Differential Pressure	±0.5 psid (±3.4 kPa)	Same as sensor

PDC SIMULATION OF STEADY-STATE CONDITIONS

The simulation of steady-state conditions in the IST was started by simulating the performance of each individual component, such as a heat exchanger or a turbine. The goal of these calculations was to match the experimental conditions while maintaining as much of design information as was provided in the benchmark. If an exact match of the outlet conditions could not be obtained, the inlet conditions were varied within the selected uncertainty range in Table 1. This variation is not only acceptable; it was expected to be required in some cases. For example, the discussion above demonstrated that the variation of inlet/outlet conditions is required for all heat exchangers in order to obtain a heat balance. Since the calculations described in this chapter are done with the steady-state part of the Plant Dynamics Code, a perfect heat balance between two sides of a heat exchanger facilitates meaningful testing of the code modeling.

If the experimental results could not be matched even within the uncertainty range of the fluid conditions, some variation in the input for the design parameters was introduced. Of course, the goal was to minimize such changes. In the case of the recuperator, however, a few variations in the design parameters were expected given that only limited information on the recuperator design is available. In any case, whenever the changes are made to the design, they are made only once. Design variations to match conditions at different points in the test run were not allowed.

Heat Exchangers

The oil-to-CO_2 intermediate heat exchanger (IHX) and CO_2-to-water precooler are shell-and-tube heat exchangers for which all information needed for PDC modeling is available. The PDC shell-and-tube heat exchanger model was extended to include the effects of the baffle plates on the shell side pressure drop, using a model previously developed by ANL for the analysis of sodium heat exchangers. The results of stand-alone calculations for these heat exchangers show that good agreement is achieved on the CO_2 side in terms of the outlet temperature and the pressure drop. There are some differences in the oil and water outlet temperatures, but these differences are close to the adopted measurement uncertainty in Table 1. There is a significant difference in the pressure drop prediction on the oil side of the IHX, which is most likely due to assumed parameters for the baffle plates. Since the oil side pressure does not affect the CO_2 side in any way (oil properties are not pressure-dependent), no further analysis was carried out to investigate the reason for this difference in the pressure drop on the oil side and/or refine the baffle plate design to match that pressure drop.

Since little information on the recuperator was provided by BMPC (even the heat exchanger type was not specified), accurate modeling of the recuperator is not considered a part of this PDC validation effort. The recuperator is only modeled to the degree sufficient to provide the correct conditions to the cycle calculations. Since the IST drawing shows the recuperator as a rectangular heat exchanger, a PCHE configuration was assumed for PDC modeling. The design parameters were selected to match whatever information is available limited specifications.

The results for the recuperator calculations showed that the measured outlet temperature on the hot side is matched well (within 0.2 °C). The pressure drops are close, although there is slight overestimation on both sides (between 5 and 8 kPa). There is a significant difference in the cold-side outlet temperature, 189.3 °C in the experiment vs 186.8 °C in the PDC calculations. However, due to a significant difference with the IHX-inlet temperature just downstream of the recuperator-outlet location, there is doubt that the recuperator-outlet temperature on the cold side was measured correctly. Therefore, not matching this temperature is not a concern at this moment. Also, because of the uncertainty in the cold-side outlet temperature, it is not possible to finalize the recuperator model with stand-alone calculations. As mentioned above, the recuperator model should provide accurate conditions for the cycle calculations. Therefore, other refinements to the recuperator model were carried out when the entire loop is modeled, both in steady-state and in transient, as described below.

Turbomachinery

In the previous work on the SNL loop (Moisseytsev and Sienicki, 2015), it was discussed how the radial turbines used in the experimental loops are not prototypical of the full-scale cycles (e.g., 100 MWe output), where an axial turbine design is better suited to achieve high cycle efficiency. Therefore, validating the radial turbine models in the PDC is not as important as for the other components for code calculations of full-scale systems. Consequently, the empirical correction factors, specific to the SNL loop, were introduced in the turbine performance subroutine to match the turbine performance for the entire loop simulation. The IST experiment employs the same radial turbine design; therefore, the same logic for code validation would be applicable to this experiment meaning that a simple empirical correction factor would be sufficient as long as the turbine performance is predicted accurately over a wide range of experimental conditions.

As with the SNL loop, the direct code application to the experimental conditions without any corrections resulted in significant differences between the code predictions and the data. For example, the code predicted 11.195 MPa for the generator turbine outlet pressure, compared to the measured 10.051 MPa, for 7000 seconds conditions. However, it was found that the code results are extremely sensitive to the input parameter of the nozzle throttle distance. For example, changing this input from the nominal value of 4.2 mm to 3 mm (about a 1 mm change) changed the outlet pressure at 7000 seconds conditions from 11.195 MPa to 9.805 MPa. Therefore, it was possible to match the experimental data with the nozzle throttle distance changed by less than 1 mm. Note that the IST benchmark information refers to as-designed, not necessarily as-fabricated, conditions, although it is believed that fabrication tolerances will be better than a 30% change in the throttle distance. More importantly, the design information does not cover as-tested conditions. It is stated in Clementoni and Cox, 2014b that erosion and bending of the nozzle tips was observed in both IST turbines. These conditions were not present during the test analyzed in this paper, but it is possible that the tested turbine configuration was at least somewhat different from the design. A small change in the distance between the nozzle blades may well be a result of blade bending, since the nozzle throttle coincides with the tips. Also, it is possible that some buildup of debris could occur in tests on the nozzle surfaces further reducing the throttle distance. The results of this sensitivity study show that not much buildup and bending are needed to significantly change the turbine performance. For the same reasons, the blade surface roughness of 1.5 μm specified by the manufacturer, Barber-Nichols Incorporated (BNI), may not reflect the as-tested roughness. It was found that increasing the surface roughness to 15 μm and decreasing the throttle distance to 3.29 mm for the generator turbine and to 3.35 mm for the compressor turbine provided agreement of the code prediction with the experimental data for both 346 and 7000 seconds time points. Since these results were obtained under input modified from the manufacturer specifications, they do not necessarily validate the radial turbine performance subroutines in the PDC (unless it could be proven that those changes reflect the actual as-tested conditions). However, as discussed above, validating the radial turbine subroutines is not important for the analysis of full-scale S-CO_2 systems. The significance of these results is that they are obtained without any empirical correction factors.

Matching the IST compressor performance has proven to be more challenging than for the turbines. No simple design modifications were found that would provide agreement across the operating range of the compressor even for the single test analyzed in this work. One of the reasons for this difficulty is believed to be the uncertainty in the experimental data for the inlet conditions which is more important for the compressor near the critical point than for the turbines. The measured and corresponding CO_2 properties at the compressor inlet conditions are demonstrated in Table 2 (the difference between the locations of pressure, temperature, and density sensors are believed to be small and are ignored in Table 2). The measured values are shaded in Table 2; unshaded values are calculated from CO_2 properties. As Table 2 shows, all three measurements are not consistent, since when any pair of measured values is used, the calculated third value is different, and significantly so, from the measured value. Since the temperature is believed to be the least accurate measurement, for further analysis in this paper it is assumed that the pressure and density provide a more accurate indication of the actual conditions. This approach is similar to the previous analysis of the SNL loop. However, it needs to be noted that the IST conditions are further away from the critical point, such that the uncertainty in the density measurements may be more important than the uncertainty in the temperature measurements for defining the actual conditions. Therefore, even though the pressure-density pair in Table 2 is selected for further analysis, there are reasons to believe that all three measurements most likely need to be varied, hopefully within the uncertainty range, to calculate the actual IST compressor inlet conditions.

Table 2. Compressor-Inlet Conditions at 7000 s

Conditions	T, °C	P, MPa	ρ, kg/m^3
Measured T and P, calculated density	36.3	9.798	684.8
Measured P and density, calculated T	**35.65**	**9.798**	**695.1**
Measured T and density, calculated P	36.3	10.02	695.1

Calculations with the PDC compressor performance subroutine showed that the code undepredicts the compressor performance, meaning that the calculated values for the outlet pressure and temperature are lower than the experimental values. The agreement of the performance predictions improved significantly when the following corrections were introduced to the compressor performance subroutine:

- Total (not static) pressure and temperature at the compressor outlet are compared with the experimental data,
- Disk friction losses are added to the enthalpy rise in the impeller,
- Effective aerodynamic blockage from boundary layer effects at the impeller outlet was limited to 10% of the flow area.

Even with these changes, conditions at different points in the test could not be matched perfectly, as shown in the Table 3, "(no correction)" columns, although the differences only affect the third digit of the values. While the outlet pressure is overpredicted at 346 s, it is underpredicted at 7000 s. It was then found that the prediction could be improved if a correction factor of 0.87 is introduced to the as-calculated diffusor loss coefficient (this correction means that the actual diffuser loss should be 13% smaller than currently calculated). The new results, shown in Table 3, "(with the 0.87 correction)" columns, demonstrate almost perfect agreement (to the fifth digit of the value) across all considered conditions in the experimental run.

Table 3. Performance Prediction of Compressor

Time, s	Experiment		PDC Results (no correction)		PDC Results (with 0.87 correction)	
	Temperature, °C	Pressure, MPa	Temperature, °C	Pressure, MPa	Temperature, °C	Pressure, MPa
346	40.1	11.415	39.7	11.565	40.0	11.412
1030	42.2	12.535	41.7	12.555	42.0	12.538
7000	45.4	14.278	44.9	14.189	45.0	14.273

Other Components

In the PDC, the valves are approximated by a sudden contraction in the flow area in the pipe immediately followed by a sudden expansion back to the full pipe flow area (Crane, 1988). In this treatment, the fully open valve poses no flow area change and the pressure drop through the open valve will be zero. However, among the benchmark specifications provided by BMPC, the manufacturer data for the valves were also provided. In the design data, one of the fields is the flow resistance of the open valve reported in the form of the valve coefficient, C_v. Therefore, to include the manufacturer information on the pressure drop for fully open valves, an additional input of the valve coefficient for a fully open valve, C_v^{open}, was added to the PDC as a user input now required for each valve. That value is used to calculate the form loss coefficient for an open valve, which is fixed in the transient and is added to previously implemented valve form loss to obtain a total loss coefficient for a valve.

BMPC provided information on the flow resistance (pressure drop) measurements for each flowmeter in the IST loop. To account for this resistance, the flow meters are modeled in the PDC as valves (named FMTGv, FMTCv, and FMCv) with the open valve coefficient input calculated to match the measured pressure drop at the specified flow conditions, as described in the previous section. For all IST flowmeters, the equivalent valve coefficients are calculated to vary between 58.43 and 59.12, so a single value of $C_v^{open} = 59.0$ is used for the PDC calculations of the pressure drop through the flowmeter "valves." These valves are assumed to remain fully open during the tests, such that the pressure drop through them is automatically re-calculated by the PDC for changing flow conditions with a fixed form loss coefficient.

The input for pipes (diameter, length, number of bends, bend radius) was taken from the provided piping layout. There were only two changes made to the actual design information. First, each flow split (i.e., tees) was simulated as two bends, to approximately provide the same pressure drop (Crane, 1988). Also, each heat exchanger has a welded connecting pipe piece which was not included in the loop piping sections. The lengths of the extra pipe sections were estimated from the component drawing and were added to the corresponding pipes. Also, initially, perfect insulation on the pipes was assumed. That input was later changed, as described below, to provide better agreement with the measurements.

Steady-State Simulation of the Entire Loop

The first application of the steady-state part of the PDC to the IST conditions at 7000 seconds showed good overall agreement with the experimental data. At the same time, some differences were identified and further analysis was carried out to resolve those differences. It was realized, though, that they are minor issues, so no significant changes to the input files and/or the model were warranted just to address these differences and degrade the agreement elsewhere. These differences are discussed below:

1. *Heat loss between IHX and turbines*. A temperature loss of 1-1.5 °C is consistently observed in the experiment, but not supported by the calculated temperature loss from the PDC results. While this difference is still within the measurement uncertainty range in Table 1, the code results were obtained using an idealized assumption of perfect insulation and thus can be improved by adding realism to better match the test data. Stand-alone calculations of heat losses from the insulated pipes, assuming a 7.6 cm (3") insulation thickness and 0.04 W/m·K thermal conductivity resulted in less than 0.2 °C temperature drop in these pipes, which is still smaller than in the experiment. A parametric study on the heat loss from the IHX-TurbG line to attain ~1°C temperature change was carried out. It was found that if the insulation is assumed to reduce the heat loss by 80% (bare pipe heat loss multiplication factor for the PDC input for Pipes 1-3 is k_HL=0.2), the temperature change between the IHX and turbines is close to the experiment. Since the IST loop uses similar insulation on all pipes, the same 0.2 factor was applied to all pipes in the PDC model.

2. *Consistent lower pressure at the compressor turbine (TurbC) inlet in the experiment, compared to generator turbine (TurbG) inlet.* There is a small difference in the piping run lengths from the flow split point to two turbines, but this difference and the frictional pressure drop are too small to explain the 9 kPa difference in measured pressures. To match the difference of 9 kPa between the TurbC and TurbG inlet pressures, the TurbC throttle valve coefficient for an open valve was reduced to 43 (compared to 60 before and for TGv).

3. *Compressor flow rate is higher, while turbine flow rates are lower in the PDC than in the experiment*. This discrepancy may be a result of implementation of the leakage and thrust balance flows. An effort was made to include the unmeasured thrust balance flow taken from the precooler outlet and supplied to the TurbG shaft into the model similarly to the leakage flow. It was quickly realized, though, that addition of a pump would be required to simulate a flow in the correct direction, further complicating the modeling. Therefore, this thrust balance flow is not currently included in the PDC IST model.
4. *Temperature drop between the recuperator and IHX*. This issue was already discussed above. It appears that the recuperator outlet temperature measurement is too high. The IHX inlet temperature measurement seems to be more realistic.
5. *Heat balance on the IHX hot (oil) side*. The code predicts a 7% lower flow rate and heat duty than the measurements. A much better agreement on all temperatures was achieved by further fine-tuning the nozzle throttle distances for the two turbines (this time, only within 0.05 mm) and the heat transfer fin efficiency for the recuperator (from 0.9 to 0.85).
6. *Water flow rate in the precooler is overpredicted by the code by about 15%*. This overprediction was addressed by reducing the input for the inlet water temperature within the measurement uncertainty in Table 1 by 1 °C.
7. *Somewhat smaller pressure drop in the loop.* This difference is believed to be a result of not including heat exchanger headers pressure drops in the model. It was addressed by introducing an artificial valve at the recuperator outlet with a valve coefficient, C_v=50.

The steady-state PDC results with all the adjustments described are shown in Figure 2 in comparison with the measured test data at 7,000 seconds. Overall, the results in Figure 2 demonstrate agreement of the PDC results with the experiment. It appears that no further adjustments to the PDC model are needed at this point and the calculations can proceed to the comparison of transient results with the data.

TRANSIENT SIMULATION

Initial Conditions and Simulation Time

The transient calculations in the PDC start from steady-state conditions. The steady-state calculations, described in the previous chapter, could not be used for this purpose since they occur at the end of the tests. The benchmark specification provides data starting at time=0 and does not describe operations prior to that time. It is obvious from the data that some loop operation occurs prior to the reported time=0. BMPC has confirmed that the system was at steady-state conditions for 1200 seconds prior to this data set. Therefore, time=0 was selected as a starting point for the transient calculations, although the conditions at that time may be somewhat further from ideal steady-state conditions than those at 7,000 seconds simulated above.

The experiment was run for 7,000 s, although only first 3,500 seconds include some form of transient. The time after 3,500 seconds was devoted to obtaining steady-state conditions and is of little interest for comparing PDC transient results with the data. For example, the heater inlet temperature does change slightly between 4,000 and 7,000 seconds, but this change is limited to about 2 °F (1°C). At the same time, running a transient calculation to 7,000 seconds would double the PDC computational time. Therefore, it was decided to limit the PDC transient simulation to the first 4,000 seconds of the experiment.

Transient Definition

In the PDC, the transient is defined by the input to external variables, such as changing boundary conditions and operator actions. The input variables, relevant to the IST test simulation, include:

- *Shaft Speeds.* In the PDC simulation of the IST, the shaft speed automatic control is not currently simulated. Instead, the measured shaft speed is directly supplied to the PDC as an input variable as a table of values versus time. With this approach, spikes in the turbine-generator shaft speed when turbine-compressor shaft speed changes were introduced (the largest one at around 600 seconds and smaller ones everywhere else) are not included in the input shaft speed table and are therefore not currently simulated in the PDC.

- *Target Precooler-Outlet Temperature.* This input is provided to better match the conditions close to the critical point. Normally, this would be the direct input of the target or measured precooler outlet temperature. However, as discussed above, it was decided to rely on density and pressure measurements to define the compressor-inlet (or precooler-outlet) conditions. So, the target precooler-outlet temperature for the water side control is calculated based on the measured pressure and density at that location and then fitted with a piecewise function for the PDC table input as demonstrated in Figure 3.
- *Inlet Water Temperature.* It was found that a better agreement on the steady-state water flow rate was obtained when water temperature was reduced within the uncertainty by 1 °C. To be consistent with that approach in the transient calculations, the PDC transient input for the water temperature was also reduced by 1 °C.
- *Oil Flow Rate.* The benchmark specifications state that the oil flow rate (oil pump head) was maintained at the same level during the test. The actual data shows that although there are some variations in the flow rate, these variations are within 0.5% of the steady-state value. Therefore, a constant oil flow rate of 23.1 kg/s can be assumed for the PDC input.
- *Target IHX Outlet Temperature.* In the IST, the CO_2 IHX outlet temperature is controlled by means of the oil heater power. The benchmark specifications say that for this test the target temperature was 282.2°C (540 °F), but also suggest that the actual temperatures are 0.6 °C (1 °F) higher. The measured IHX outlet temperature demonstrates that the temperature is indeed maintained around 282.8 °C. Therefore, the PDC input for this temperature is set equal to the constant value of 282.8 °C.
- *Compressor Recirculation Valve.* As described above, the compressor recirculation (CR) valve position in the IST experiments is defined by the lookup table versus the commanded compressor speed. Since the speed is an operator input, the valve position is also an input versus time. As discussed above, the PDC implements a simplified treatment of the valves. As a result of that simplification, it is expected that the PDC valve position would be different from the actual valve position. This proved to be the case for the CR valve. For example, the CR valve is about 70% open at time=0 during the experiment. At the same time, the simplified valve loss coefficient treatment in the PDC resulted in a calculated valve open fraction of about 3.5%. Notice that these two values refer to different characteristics. The IST valve position is the fraction of valve full movement, while the PDC valve position is the fraction of pipe total area open to the flow at the valve throttle. To account for this difference, a relationship to transform the actual valve position into the would-be PDC valve open fraction was developed. That relationship was obtained by using the IST data at three different times (and valve positions) during the experiment and calculating what the PDC valve open fraction would be for the given inlet conditions, flow rates, and pressure drops. Another point was obtained assuming that a fully closed valve means zero flow area in both cases. The four points were then fitted with a polynomial, and that fit was used to obtain the PDC input for the CR valve position in the transient. The accuracy of this treatment of the CR valve and the relationship between the actual valve position and the current PDC approximation will be verified by comparing the PDC prediction of the flow rate through the valve with the experimental data.

Loop Control

The IST oil heaters are operated in an automatic control mode to maintain a target CO_2 temperature at IHX outlet. This setup is similar to the electric heater control used in the SNL loop and previously implemented in the PDC. In the SNL loop simulation, the electrical heater power was directly applied to the tubes; in the case of the IST, this power is applied to heaters to heat the oil. Since the complete oil loop, including heaters, is not simulated in the PDC, the CO_2 temperature control was modified to maintain the CO_2 IHX outlet temperature by means of changing the oil temperature at the IHX inlet.

Because in this approach the heater response is assumed to be instantaneous, a limit on the heater power change (which is actually an oil temperature change) of $\pm$1%/s was initially used for the PDC transient calculations. This limit was then adjusted, together with the PID coefficients, to obtain a heater response close to the IST measurement, as described in the next section.

In the PDC simulation of the IST, two automatic controls are implemented to simulate actual loop operation: oil heater power and water flow rate. Since the characteristics (PID coefficients, rates of change, etc.) of the actual control setups in the experiment were not provided initially with the benchmark, the PDC input for these controls were changed to obtain responses at least close to the experimental setup.

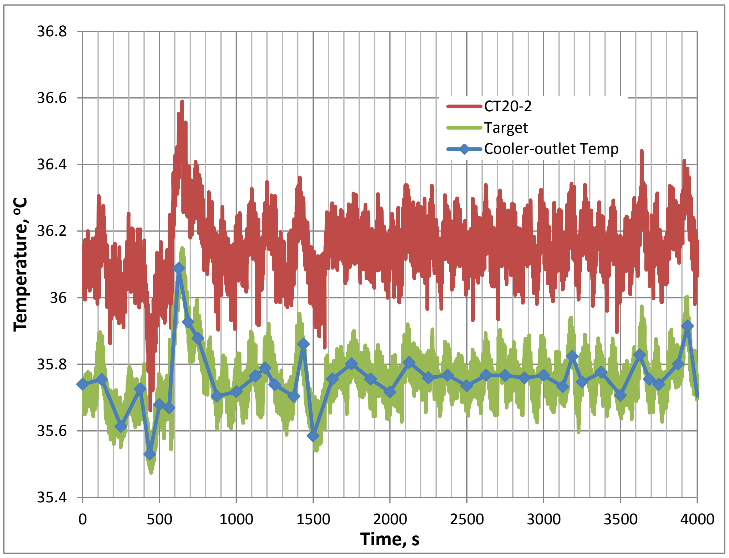

Figure 3.Target Precooler-Outlet Temperature.

First Transient Results

The first transient results showed that the general trends in all calculated variables are predicted correctly by the PDC. Also, some PDC results match the data almost perfectly. All of the calculated temperatures and flow rates were very close to the experimental values for the entire transient. However, there are some differences in other results, which are sometimes significant.

The pressure and compressor-inlet density results show perhaps the most significant difference between the code predictions and the data. Figure 4 shows the results for the density at the compressor inlet. In this and the following figure, the test data is shown as a solid (dark blue) line with the uncertainty range from Table 1 (“Total Uncertainty” column) shown as a (light blue) band, while the PDC code prediction is shown as a (red) line with a marker symbol. Shortly after the transient starts, the test data show increases in density as well as both high- and low-side pressures, which are not captured in the code results. An investigation was carried out to find the reasons for this difference.

CO_2 Inventory Conservation

The comparison of the PDC results with the experimental data shows that while the majority of the PDC results agree well with the test, something is going on with the CO_2 pressure and density changes during the experiment. Those changes are not calculated by the code, so it predicts lower pressures and densities for the majority of the transient, although the steady-state results for time=0 show better agreement.

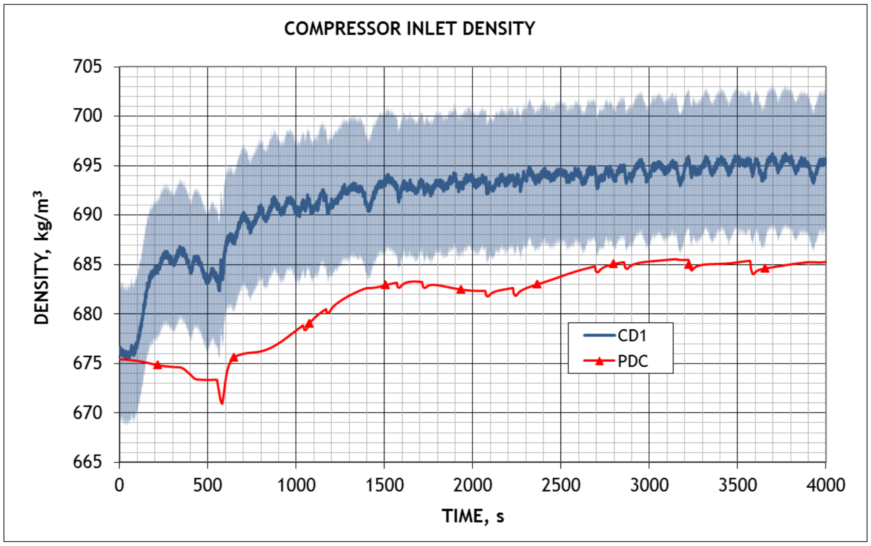

Figure 4. First Transient Results for Compressor-Inlet Density.

It is stated in the test description that the turbomachinery cavity pressure set point was changed from 400 psia (2.76 MPa) to 300 psia (2.07 MPa) at 78 seconds. This change in cavity pressure (and mass) after 78 seconds also means that some CO_2 mass was being pushed from the cavity leakage system into the main loop and thus explains why the system pressures and densities (in Figure 4) start to diverge around 100 s. Since the PDC model includes a simplistic representation of the cavity leakage flow without any pumps, it could not currently represent this change in cavity pressure and CO_2 mass.

This change in CO_2 inventory is also confirmed by comparing the PDC steady-state results at time=0 with the steady-state calculation for 7,000 seconds. The PDC calculates the total CO_2 mass in the cycle (in components, inlet/outlet plena, and piping) to be 235.7 kg at time=0, but 239.4 kg at 7,000 seconds. In other words, in order to obtain steady-state conditions at 7,000 seconds starting from the conditions at time=0, 3.7 kg of CO_2 *would have to have been* added to the cycle.

In order to see if this change in CO_2 mass is responsible for the loss in agreement on pressures, another set of steady-state and transient calculations was carried out. Future PDC model updates might include an accurate simulation of the leakage collection system (with its pumps and their characteristics and all piping and volumes), but in this study, a more simplified analysis was carried out. In this analysis, the conditions (PDC input) at time=0 were adjusted to match the CO_2 mass at 7,000 seconds (239.4 kg). The simplest input adjustment to match the mass was to increase the compressor inlet pressure, while conserving all other inputs. It turned out that this pressure needs to be increased from 9.4 MPa to 9.635 MPa to obtain the 239.4 kg CO_2 inventory at steady-state.

Transient Results with Higher CO_2 Mass

The transient calculations with the same external input (described above) were repeated with the PDC. No new changes for the transient input were introduced. Therefore, the higher initial compressor-inlet pressure in the steady-state input remains the only difference from the previous transient simulation.

Some transient results for this simulation, in comparison with the test data, are shown in Figure 5. As expected, the agreement on pressures and densities earlier in the transient is worse than before. However, starting from around 350 s, i.e. for about 90% of the transient, both the high and low pressures are predicted much more accurately. The same behavior is observed for the compressor-inlet and generator turbine outlet densities; after 600 s, the agreement is good. The prediction on the CO_2 flow rates is also very good. After 600 s, the agreement on all flow rates is almost perfect. Good agreement on the compressor recirculation flow rate also confirms the correct modeling of the CR valve in the PDC.

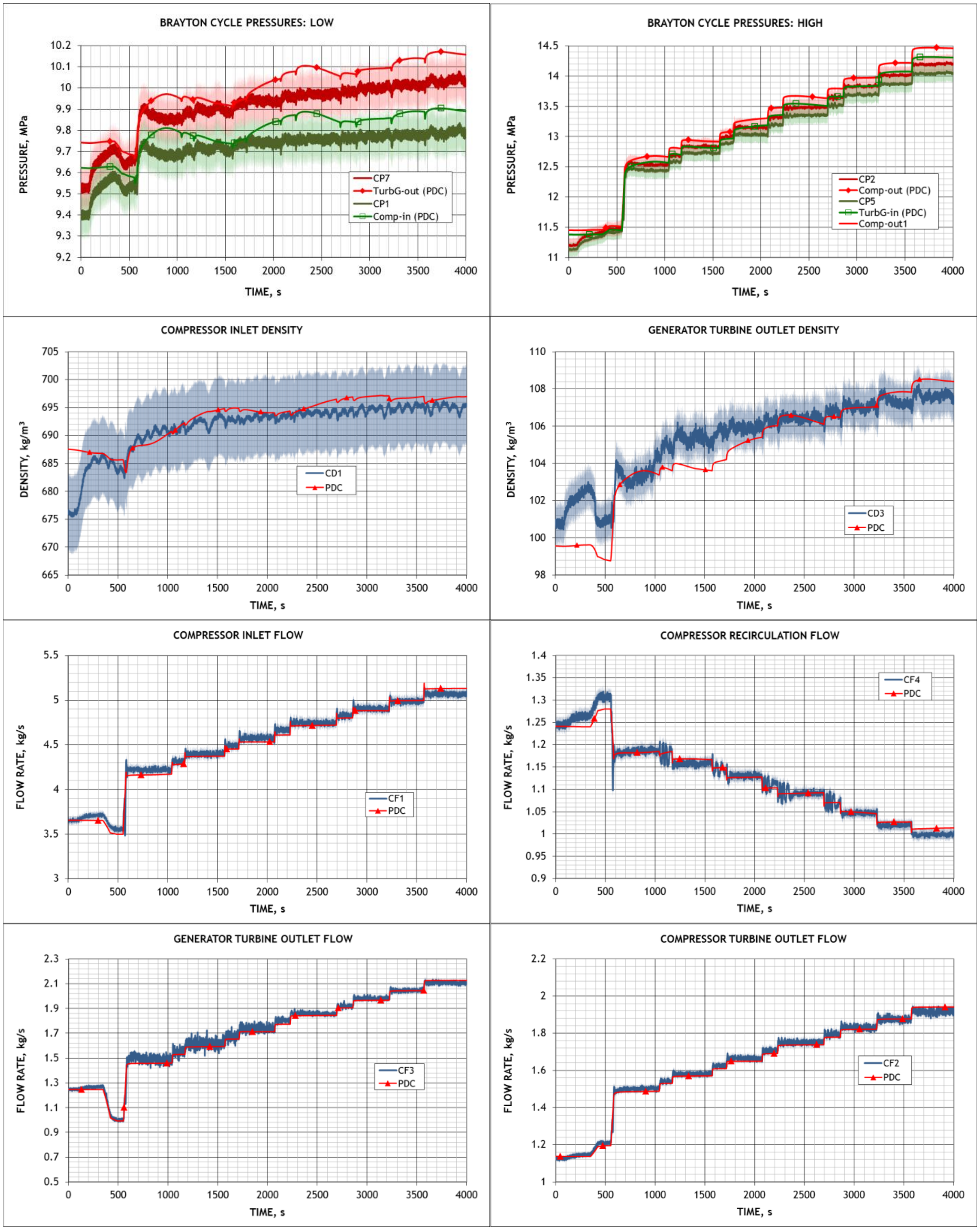

Figure 5. Comparison of Experimental Data with PDC Transient Results with Higher CO_2 Mass.

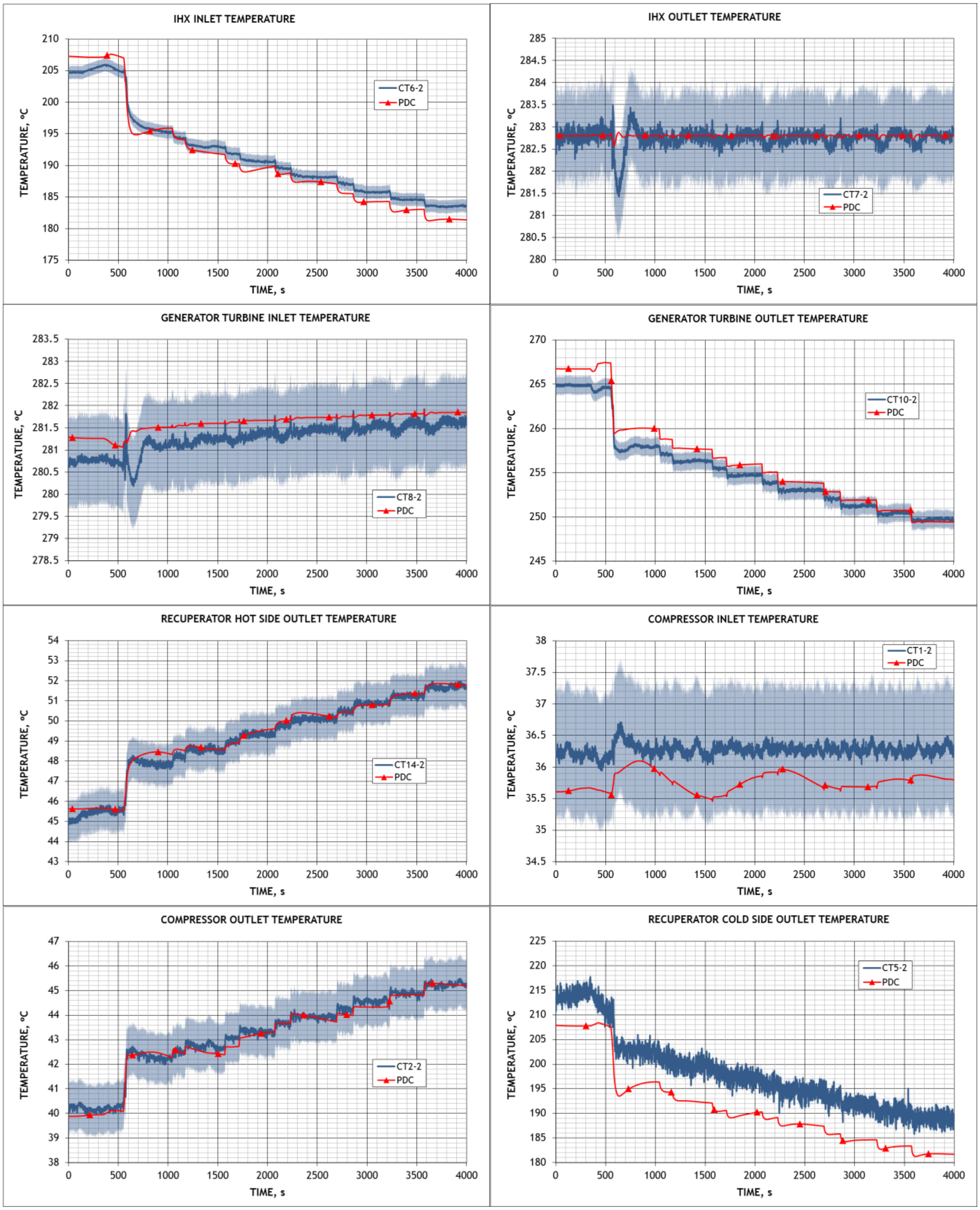

Figure 5. Comparison of Experimental Data with PDC Transient Results with Higher CO2 Mass. (Continued)

The IHX inlet temperature is underpredicted during the majority of the transient. These results might be improved in the future with further refinements in the recuperator model. The IHX outlet temperature seems to be controlled better by the PDC control setup than in the test, but this result is attributed to not modeling all of the spikes in the shaft speeds and the corresponding spikes in the CO_2 flow rates. Both turbine inlet temperatures are consistently overpredicted by the code which might suggest that they are due to underpredicting the heat loss in the pipe insulation. However, the difference between the PDC results and the data is small, less than 1 °C. Both turbine outlet temperatures and the recuperator inlet temperature are predicted well, especially later in the transient. The recuperator outlet temperature on the hot side and the precooler inlet temperature are predicted very accurately. Both the calculated precooler outlet temperature and compressor inlet temperatures differ from the data. However, this is the result of the cycle control setup in the PDC. These temperatures were set to be adjusted to match densities in these locations. Still, the differences stay within 1 °C. The compressor outlet temperature prediction is almost perfect. However, the recuperator inlet temperature is the same temperature in the PDC results but is higher in the experiment. The reason for this difference in the experimental data is still unknown; it could be just the result of measurement uncertainty. The recuperator cold side outlet temperature is lower in the code results and well outside the uncertainty margin. This result, together with the steady-state results discussed above, further confirms the suspicion that this temperature was not measured accurately in the test.

The results in Figure 5, combined with the results earlier in the transient in Figure 4 do confirm the CO_2 inventory change in the cycle resulting from the cavity pressure control action. For future calculations, the effect of this action could be simulated with some sort of inventory control action (or the entire leakage collection system could be simulated). However, at this point, the agreement for the majority of the transient in Figure 5 for all calculated values confirms the ability of the PDC to simulate at least this selected IST test. In future work, other IST tests will be simulated with the PDC to see if the agreement also holds for other tests and conditions.

SUMMARY

The ANL Plant Dynamic Code continues to undergo testing, improvement, and validation through comparison with data from integral S-CO_2 cycle demonstrations at SNL and BMPC. The most recent addition to available S-CO_2 test data is data obtained at the Integrated System Test constructed and operated by BMPC. Relative to data from the SNL RCBC loop received thus far, data from the BMPC IST demonstration provides several benefits for code validation including a different closed Brayton cycle configuration, fully thermally insulated piping and components, longer-term and better data approaching a steady state, better defined boundary conditions, simpler heat addition and heat removal heat exchanger designs, and more instrumentation, including differential pressure sensors across components. The IST has also been operated in a regime further away from the CO_2 critical point than the RCBC has which reduces the magnitude of some effects resulting from property variations near the critical point such that other effects can manifest themselves more unambiguously.

As experience continues to be gained and lessons are learned from applying the code to small-scale integral S-CO_2 cycles, an approach for how to effectively test and validate the code is emerging. The small-scale tests involve additional processes and phenomena that are negligible for full-scale S-CO_2 Brayton cycles (e.g., at a 100 MWe output level). It is necessary to extend specific code models especially for turbomachinery to account for design features of the small-scale components. The need to account for leakage flows from turbomachinery and their reinjection into the loop flow is one example. There is a need to model the flowpath for leakages, their collection, and reinjection using piston pumps. Multinodal modeling of that flowpath isn't currently implemented in the code but an attempt to account for the effects of leakages has been made through simple modifications of the code models for the main loop configuration. The code should ideally model the experiment facility control system such that it simulates the various controllers that seek to maintain target conditions; that is, the code should model the facility with its control system. An attempt is made to model specific controllers. However, the PID coefficients for the facility controllers are not available and other sets of PID coefficients have to be assumed to simulate the anticipated controller behavior. Similarly, an attempt is made to simulate hardware that effects control actions such as valves including their effects on pressures around the loop.

Testing and validation is not as straightforward as simply comparing code calculations with data. This is because all data incorporates some uncertainty. The IST test data exhibits a significant statistical uncertainty that exceeds that expected for the basic individual sensors. Significantly, the level of comparison between calculation and experiment is sometimes quite precise involving differences in the third, fourth, or even fifth digit of the variable in question. To achieve a meaningful comparison at such a level of precision, it is sometimes necessary to assume slightly different values than the recorded measurements. When data values are thus changed, the changes are carried out to maintain consistency between temperature, density, and pressure according to the NIST equation of state for CO_2, or changes are kept within the observed uncertainty ranges. It is expected that in the former case forcing consistency with the equation of state improves the data for CO_2. The component models are one-dimensional and, at least in some cases are empirical, and sometimes depend upon parameters that cannot be straightforwardly related to the component design. This is particularly the case for the turbines and compressor. It is found that some parameters need to be changed to better simulate the observed component performance. This is not surprising given the simple nature of the modeling. Thus, showing that the code predictions agree satisfactorily with the data involves modification of both the code modeling and the data within the limits of uncertainty. A key question for the future is whether the present parameter modifications will continue to be appropriate for the analysis of future tests at different conditions.

The P1-S2-63264-CC_7000s test was modeled and analyzed. The experiment consists of several step changes in the turbomachinery shaft speeds followed by long-term steady-state operation. This test was selected for code testing and validation because it provides steady-state data following the transient, which was extremely useful in first refining the models for each component, especially the heat exchangers, in order to reduce uncertainties in the input and improve the modeling of components.

The PDC modeling of the IST test thus started with the steady-state simulation of performance of each component and the entire loop following the transient portion of the test. It was found during this stage that although the IST data from the subsequent steady-state phase is an effective means to modify both models and data, this does not bring about perfect agreement or eliminate uncertainty altogether. Several features of the measured data were identified which complicate the accurate modeling and performance prediction of the components and the entire loop. The most important such features include: inconsistency between the measured pressure, temperature, and density at the compressor inlet; inconsistency between the recuperator outlet and IHX inlet temperatures; not obtaining a perfect flow balance around the loop; lower than expected measurement of the compressor outlet density; and lack of perfect heat balance for all heat exchangers.

On the modeling side, several adjustments had to be made to improve the prediction of the steady-state IST data. Some adjustments, such as reducing the nozzle throttle distance in the turbines, might, at least to some degree, represent the actual operating conditions. The other adjustments, however, are purely artificial and tuned for the IST loop. An example of such an adjustment is the correction factors for the compressor diffuser loss coefficient which was found to improve the prediction of compressor performance but has little theoretical basis. In addition, the input for the recuperator had to be at least partially invented because limited information on this heat exchanger design was provided. However, these adjustments were kept to a minimum and were not changed once satisfactory steady-state results were obtained. For example, there were no extra corrections implemented between the steady-state and transient simulation. Also, in some cases, no adjustments at all were needed to achieve satisfactory agreement with the test, as was the case for the IHX and precooler.

For the transient simulation with the PDC, the boundary conditions which define the operator actions during the test were provided to the PDC. The oil side control was simulated by automatic oil IHX-inlet temperature control to maintain the target CO_2 temperature at the IHX outlet. The water flow control was used to maintain the CO_2 conditions at the precooler outlet. Both of these controls were optimized in the PDC to obtain a response close to the experimental results. In addition to these controls, the other inputs for the transient definition were the oil flow rate, water inlet temperature, turbomachinery shaft speeds, and the compressor recirculation valve position. For this valve, a simple correlation was successfully developed to relate the actual valve position to the flow open fraction used in the PDC.

The first results of the transient simulation showed agreement with the test data earlier in the transient. However, after about 100 seconds (out of a 4,000 seconds transient), both pressures and densities started to deviate from the test data, although the temperatures and flow rates continued to show at least acceptable agreement with the data. Further analysis revealed that this difference was caused by reinjection of a small CO_2 mass into the main loop from seal leakage in the turbomachinery. Since the cavity leakage flow system is not currently simulated by the PDC, this CO_2 mass movement could not be simulated with the current model. However, comparing the PDC results of the steady-state calculations at the beginning and the end of the transient confirmed that about 4 kg of CO_2 (compared with a subsequent total of 240 kg) shifted into the main loop during the test.

To observe the effects of this CO_2 mass change in the cycle, the transient calculations were repeated, but this time the initial conditions were adjusted to match the CO_2 mass at the end of the test (rather than at the beginning). The new PDC results indeed show much better agreement with the test for the majority of the transient, after the cavity pressure adjustment was completed. For at least 90% of the time, pressures and densities show agreement with the data. With few exceptions (which are believed to originate from the measurement uncertainties), the temperatures also agree with the experiment within 1 °C or less. The flow rate agreement is almost perfect. The oil temperature and water flow rate also show agreement with the test for the entire transient.

Overall, both the steady-state and transient PDC results for the IST simulation are judged to be satisfactory and confirm that the code modeling of the components and integrated cycle layout provide a good simulation of the facility. The future work in this area will be focusing on simulating other transients to see if similarly good agreement can be obtained for different cycle conditions. Also, further model improvements can be introduced to address the remaining differences. Examples of such possible model improvements including: more detailed modeling of the seal leakage collection system to more accurately calculate the CO_2 mass distribution during the tests; and more realistic simulation of system controls, including those not currently simulated in the PDC, such as automatic shaft speed and the compressor recirculation valve controls.

REFERENCES

Clementoni, E.M. and Cox, T.L., 2014a, "Steady-State Power Operation of a Supercritical Carbon Dioxide Brayton Cycle," *4th International Symposium - Supercritical CO_2 Power Cycles*, Pittsburgh, Pennsylvania, September 9-10.

Clementoni, E.M. and Cox, T.L., 2014b, "Practical Aspects of Supercritical Carbon Dioxide Brayton System Testing," *4th International Symposium - Supercritical CO_2 Power Cycles*, Pittsburgh, Pennsylvania, September 9-10.

Kimball, K.J., 2014, "Supercritical Carbon Dioxide Power Cycle Development Overview," Presentation at *4th International Symposium - Supercritical CO_2 Power Cycles*, Pittsburgh, Pennsylvania, September 9-10.

Rahner, K.D., 2014, "S-CO_2 Brayton Loop Transient Modeling," Presentation at *4th International Symposium - Supercritical CO_2 Power Cycles*, Pittsburgh, Pennsylvania, September 9-10.

Moisseytsev, A. and Sienicki, J. J., 2006, "Development of a Plant Dynamics Computer Code for Analysis of a Supercritical Carbon Dioxide Brayton Cycle Energy Converter Coupled to a Natural Circulation Lead-Cooled Fast Reactor," ANL-06/27, Argonne National Laboratory.

Moisseytsev, A. and Sienicki, J. J., 2015, "Lessons Learned and Improvements in ANL Plant Dynamics Code Simulation of Experimental S-CO_2 Loops," PowerEnergy2015-49182**,** Proceedings of ASME Power & Energy 2015, San Diego, CA, June 28-July 2.

National Institute of Standards and Technology (NIST) Fluid Properties Website, http://webbook.nist.gov/chemistry/fluid/, 2015.

Crane Co., 1988, "Flow of Fluids through Valves, Fittings, and Pipes," Technical Paper No. 410.

ACKNOWLEDGEMENTS

Argonne National Laboratory's work was supported by the U. S. Department of Energy Advanced Reactor Technologies (ART) Program under Prime Contract No. DE-AC02-06CH11357 between the U.S. Department of Energy and UChicago Argonne, LLC. The work presented here was carried out under the Energy Conversion Technology area of the ATR Program. The authors are grateful to Gary Rochau (SNL), the Technical Area Lead, Bob Hill (ANL/NE), the National Technical Director, as well as Brian Robinson and Carl Sink (U.S. DOE), Headquarters Program Managers for the project. The authors are especially thankful to Patrick Fourspring, Kevin Rahner, and Eric Clementoni of Bechtel Marine Propulsion Corporation (BMPC) for the preparation of the IST benchmark specifications and their continuous support during the analysis presented in this paper. The authors also appreciate the support of Brian Morris and Kenneth Kimball from BMPC in sharing the IST data with ANL.